JOC Article

Nonplanar Structures of Thioamides Derived from 7-Azabicyclo[2.2.1]heptane. Electronically Tunable Planarity of Thioamides

Tetsuharu Hori,[†] Yuko Otani,[†] Masatoshi Kawahata,[‡] Kentaro Yamaguchi,[‡] and Tomohiko Ohwada*,[†]

Graduate School of Pharmaceutical Sciences, The University of Tokyo, 7-3-1 Hongo, Bunkyo-ku, Tokyo 113-0033, Japan, and Department of Pharmaceutical Sciences at Kagawa Campus, Tokushima Bunri University, 1314-1 Shido, Sanuki, Kagawa 769-2193, Japan

ohwada@mol.f.u-tokyo.ac.jp

Received September 11, 2008

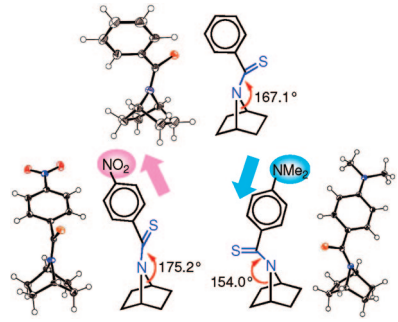

X-ray crystallographic analysis showed that *N*-thiobenzoyl-7-azabicyclo[2.2.1]heptane displays marked nonplanarity of the thioamide (**1a**, $\alpha = 167.1°$ and $|\tau| = 11.2°$) as compared with the corresponding monocyclic pyrrolidine thioamide (**2a**, $\alpha = 174.7°$ and $|\tau| = 3.9°$). In a series of *para*-substituted or unsubstituted thioaroyl-7-azabicyclo[2.2.1]heptanes (**1a**−**1h**), the planarity of the thioamide depended significantly on the electronic nature of the substituent; for example, in the *p*-nitro-substituted compound, planarity was substantially restored (**1h**, $\alpha = 175.2°$ and $|\tau| = 0.1°$). In solution, increasing electron-withdrawing character of the aromatic substituent was associated with a larger rotational barrier of the bicyclic thioamides, as determined by means of variable-temperature ^{1}H NMR spectroscopy and line shape analysis. The reduced rotational barrier, that is, reduced enthalpy of activation ($\Delta H^{\ddagger}$) for thioamide rotation, of **1a** as compared with that of **2a** in nitrobenzene-d_5 is consistent with the postulate that **1a** assumes a nonplanar thioamide structure in solution. These results indicate that the planarity of thioamides based on 7-azabicyclo[2.2.1]heptane is controlled by electronic factors in the solid phase and in solution.

Introduction

Although thioamides are analogues of amides, experimental and theoretical studies have shown that they differ from each other in many respects; the longer C═S bond and weaker hydrogen-bond-accepting ability of thioamides electronically and sterically influence neighboring groups. Also, thioamides display much higher rotational barriers about the N−C(S) bond than amides do.[1,2] Thus, thioamides have a stronger preference for planar structure than amides.[3a] An accepted interpretation of this feature is a greater contribution of the dipolar canonical structure (B) in the resonance structures (Scheme 1),[3−5] because $C_{(2p)}-S_{(3p)}$ overlap in a thioamide bond is less effective than $C_{(2p)}-O_{(2p)}$ overlap in an amide bond. Peptides containing thioamide bonds have been utilized as probes of local peptide secondary structures, but introduction of a thioamide group into a peptide linkage can have apparently contradictory effects; for

[†] The University of Tokyo.
[‡] Tokushima Bunri University.

(1) Sandström, J. *J. Phys. Chem.* **1967**, *71*, 2318–2325.
(2) Neuman, R. C., Jr.; Jonas, V. *J. Phys. Chem.* **1971**, *75*, 3532–3536.
(3) (a) Wiberg, K. B.; Rablen, P. R. *J. Am. Chem. Soc.* **1995**, *117*, 2201–2209. (b) Lauvergnat, D.; Hiberty, P. C. *J. Am. Chem. Soc.* **1997**, *119*, 9478–9482.
(4) For a counter-example to the resonance effect, see: Laidig, K. E.; Cameron, L. M. *J. Am. Chem. Soc.* **1996**, *118*, 1737–1742.
(5) Galabov, B.; Ilieva, S.; Hadjieva, B.; Dinchova, E. *J. Phys. Chem. A* **2003**, *107*, 5854–5861.

10.1021/jo801996b CCC: $40.75
Published on Web 10/24/2008

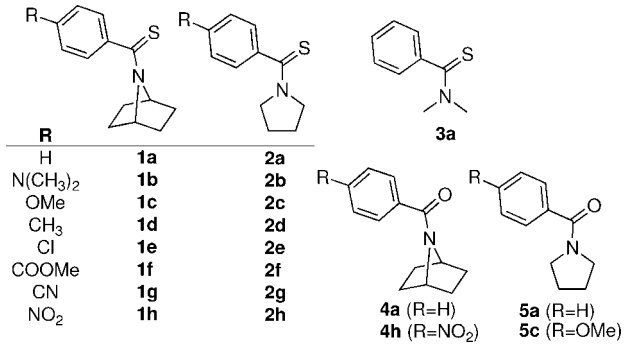

FIGURE 1. Thioamides in this study.

SCHEME 1. Resonance Structures of Amide and Thioamide

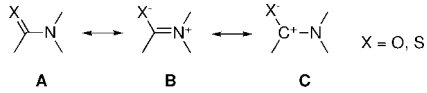

example, peptide conformations are maintained[6,7] or destabilized[8,9] due to high rotational barriers and weaker hydrogen bonding. While thioamides show a strong preference for planar structure, little has been reported about their deviation from planarity. This is an important issue in relation to the structural features of peptides containing thioamide bonds.

Bicyclic 7-azabicyclo[2.2.1]heptane amides have intrinsically nonplanar structures in the solid phase and in solution.[10,11] Thus, it is of considerable interest to know whether nonplanar thioamides can be generated from this bicyclic skeleton. In this study, the planarity of solid and solution structures of thioamide derivatives of bicyclic 7-azabicyclo[2.2.1]heptane and related amines was investigated. We found that in a series of *para*-substituted or unsubstituted thioaroyl-7-azabicyclo[2.2.1]heptanes the planarity of the thioamide can be tuned by altering the electronic nature of the substituent.

Results and Discussion

Crystal Structures of Thioamides. Various *para*-substituted or unsubstituted *N*-thiobenzamides of bicyclic (**1a**−**1h**), monocyclic (**2a**−**2h**), and acyclic (**3a**) amines were synthesized by thioxylation with Lawesson's reagent of the corresponding aroyl amides, which were synthesized by acylation of amines with suitable aroyl chlorides[11] (Figure 1 and Scheme 2). Crystal structures of some of the thioamides were elucidated by X-ray crystallography (Figure 2 and Figures S1−S9 in Supporting Information). Selected structural parameters are shown in Table 1.

The planarity of thioamide nitrogen can be represented in terms of three angle parameters, θ, α and τ, the definitions of which are shown in Figure 3: θ is the sum of the three valence angles around the nitrogen atom ($\theta = a + b + c$); the hinge angle α is the angle between the N−C(S) bond and the plane

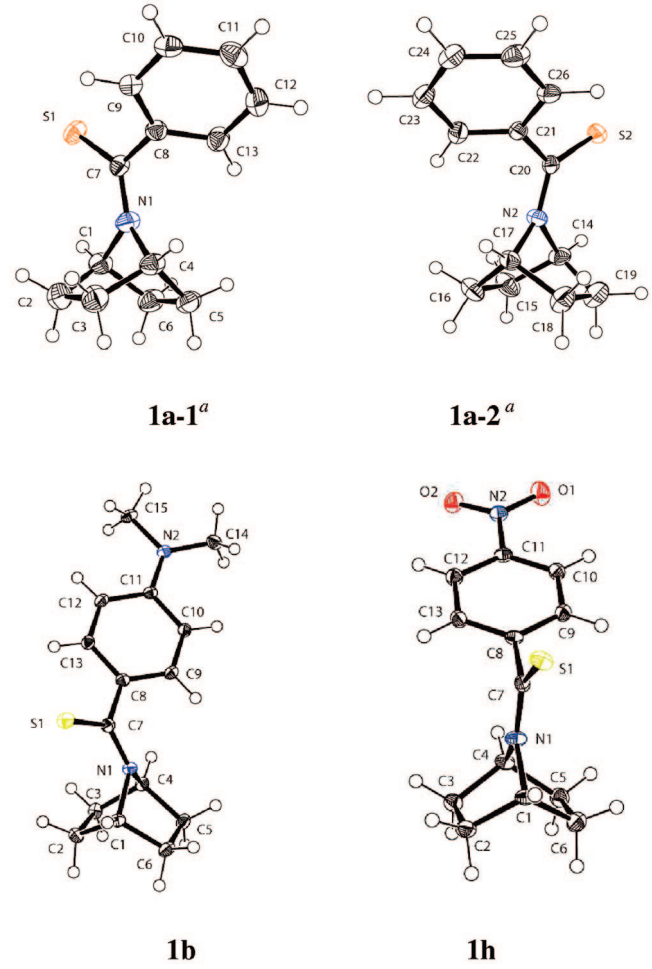

FIGURE 2. ORTEP diagrams of **1a**, **1b**, and **1h** showing the thermal ellipsoids at 30% probability. [a] Two kinds of molecules are contained in a unit cell.

SCHEME 2. Synthesis of Bicyclic, Monocyclic, and Acyclic Thioamides

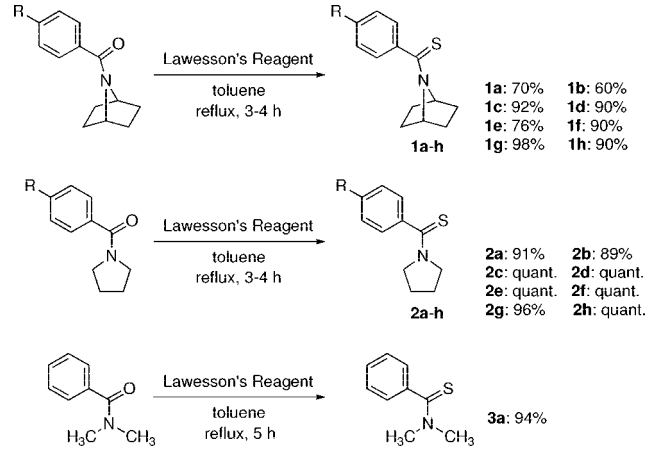

defined by the nitrogen atom, R_1, and R_2; and the twist angle $|\tau|$ is the absolute value of the mean of two torsion angles, $\omega_1(R_3CNR_2)$ and $\omega_2(SCNR_1)$ ($|\tau| = {}^1/_2|\omega_1+\omega_2|$).[12] Values of θ, α, and τ of the ideal planar thioamide are 360°, 180°, and 0°, respectively. The former two values will decrease and the third

(6) Miwa, J. H.; Pallivathucal, L.; Gowda, S.; Lee, K. E. *Org. Lett.* **2002**, *4*, 4655–4657.
(7) Sherman, D. B.; Spatola, A. F. *J. Am. Chem. Soc.* **1990**, *112*, 433–441.
(8) Artis, D. R.; Lipton, M. A. *J. Am. Chem. Soc.* **1998**, *120*, 12200–12206.
(9) Reiner, A.; Wildemann, D.; Fischer, G.; Kiefhaber, T. *J. Am. Chem. Soc.* **2008**, *130*, 8079–8084.
(10) Ohwada, T.; Achiwa, T.; Okamoto, I.; Shudo, K. *Tetrahedron Lett.* **1998**, *39*, 865–868.
(11) Otani, Y.; Nagae, O.; Naruse, Y.; Inagaki, S.; Ohno, M.; Yamaguchi, K.; Yamamoto, G.; Uchiyama, M.; Ohwada, T. *J. Am. Chem. Soc.* **2003**, *125*, 15191–15199.
(12) Winkler, F. K.; Dunitz, J. D. *J. Mol. Biol.* **1971**, *59*, 169–182.

TABLE 1. Selected Crystal Structural Data of Thioamides[a]

	R	*a* (deg)	*θ* (deg)	α (deg)	|τ| (deg)	N−C(X) bond (Å)
1a[b]	H	97.8(2)	357.6(2)	167.3	11.0(3)	1.324(2)
		98.0(1)	357.5(2)	167.1	11.2(3)	1.323(2)
1b	$N(CH_3)_2$	97.1(1)	350.1(1)	154.0	14.6(2)	1.339(2)
1d[b]	CH_3	97.6(3)	353.9(3)	159.7	12.1(6)	1.339(5)
		97.3(3)	355.7(3)	163.2	8.6(6)	1.332(5)
1e	Cl	98.2(1)	358.7(1)	170.6	12.6(2)	1.322(2)
1f	COOMe	97.8(1)	352.7(1)	157.7	9.6(2)	1.331(2)
1h	NO_2	98.6(1)	359.7(1)	175.2	0.1(2)	1.312(2)
2a	H	111.1(1)	359.7(2)	174.7	3.9(3)	1.325(2)
2c	OMe	111.2(1)	359.9(1)	176.7	5.5(2)	1.324(2)
2d	CH_3	111.1(1)	359.5(1)	173.4	5.8(2)	1.324(2)
2g	CN	111.3(1)	359.7(1)	174.8	1.3(2)	1.319(2)
2h	NO_2	111.0(1)	359.5(1)	173.7	2.0(2)	1.318(2)
3a	H	113.7(1)	359.7(1)	174.5	9.2(2)	1.333(2)
4a[c]	H	97.2(2)	349.5(2)	153.2	15.5(3)	1.356(3)
4h[b,c]	NO_2	96.9(2)	347.1(3)	150.2	13.0(5)	1.354(4)
		97.8(2)	350.1(3)	153.8	6.9(5)	1.350(4)
5c[c]	OMe	111.5(2)	359.2(2)	171.3	3.0(3)	1.345(3)

[a] Standard deviations are shown in parentheses. [b] Two kinds of molecules are contained in a unit cell. [c] Data from ref 11.

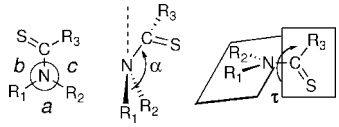

FIGURE 3. Definition of angle parameters.

value will increase as the thioamide functionality deviates from planarity to a greater extent.

As shown in Table 1, thioamides with a bicyclic skeleton (**1a**−**b** and **1d**−**f**, except **1h**) were substantially both nitrogen-pyramidal and twisted, as compared with monocyclic (**2a**, **2c**−**d** and **2g**−**h**) and acyclic (**3a**) thioamides; the α value of those bicyclic thioamides ranged from 154.0° to 170.6° and the |τ| value ranged from 8.6° to 14.6°, whereas those of the monocyclic thioamides were close to the values of planar structures (α from 173.4° to 176.7° and |τ| from 1.3° to 5.8°). In the case of the corresponding bicyclic amides (such as **4a** and **4h**), nonplanarity of the amide functionality was also observed, but the aromatic substituent effects on the planarity were insignificant, e.g., α values of 153.0° (**4a**, R = H) and 150.2° and 153.8° (average 152.0°) (**4h**, R = NO_2) (see Table 1). *N*-Aroyl bicyclic amides took nitrogen-pyramidalized amide structures, irrespective of the aromatic substituent.[11] In contrast, an electronic effect of the aromatic substituent (R) on thioamide planarity was obvious in the case of the bicyclic thioamides, i.e., the degree of planarity represented in terms of α is in the order **1h** (R = NO_2) > **1e** (R = Cl) > **1a** (R = H) > **1d** (R = CH_3) > **1b** (R = $N(CH_3)_2$). **1h** (R = NO_2) takes a nearly planar structure, whereas **1b** (R = NMe_2) takes a significantly nitrogen-pyramidalized structure (Figure 2). This trend is consistent with the idea that an electron-withdrawing group tends to restore nitrogen planarity, except for **1f** (R = COOMe).[13] This recovery of nitrogen planarity coincided with shortening of the C−N bond of these thioamides, probably due to an increase of N−C(S) double bond character. Such a phenomenon was not seen among the monocyclic thioamides (**2**) (e.g., α value 174.7° (**2a**, R = H); 173.7° (**2h**, R = NO_2)), or among bicyclic amides (**4**) (*vide ante*) (Table 1). Thus, it appears that the planarity of bicyclic thioamides can be controlled by varying the electronic nature

(13) This is due to high-density packing of **1f** with a *Z*-value of 8 and an aromatic stacking distance of 3.4 Å.

CHART 1

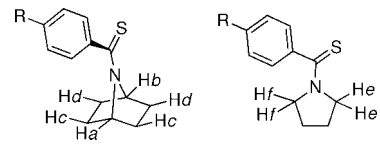

of the substituent on the aroyl group. The intrinsic nonplanarity of the corresponding bicyclic amide (such as **4a** and **4h**) was proposed to be attributable to both angle strain around the nitrogen atom (i.e., angle *a*) and 1,3-allylic strain between the bridgehead hydrogens and the oxygen atom or the phenyl ring.[11] In the case of the present bicyclic thioamides (**1**), similar structural features may also favor the observed nonplanar structures, because the C−N bond of the thioamides is shortened, as compared with that of the corresponding amides (see Table 1), imposing 1,3-allylic strain.

On the other hand, the acyclic thioamide **3a** displayed significant twisting around the thioamide bond, while nitrogen-pyramidalization was insignificant (α = 174.5° and |τ| = 9.2°).

Solution Structures of Thioamides. To estimate the N−C(S) double bond character of thioamides in solution, rotational barriers with respect to the thioamide bond, i.e., the free energy of activation ($\Delta G^{\ddagger}$), were evaluated by variable-temperature ^{1}H NMR spectroscopy in nitrobenzene-d_5 (ε = 35.6 at 20 °C) and *o*-dichlorobenzene-d_4 (ε = 10.1 at 20 °C) at 25 mM.[14,15] In variable-temperature NMR experiments, temperatures were calibrated by a standard method using an ethylene glycol.[14,16] Upon elevation of the temperature, the bridgehead proton signals (H*a* and H*b* in Chart 1) or the exo-proton signals (H*c* and H*d*) in the case of bicyclic thioamides and the α-proton signals (H*e* and H*f*) in the case of monocyclic and acyclic thioamides broadened and then coalesced. The rate constant k_c and the barriers to rotation ($\Delta G^{\ddagger}_c$) about the C−N bond in the thioamides were therefore obtained by the coalescence method on the basis of the difference in chemical shifts ($\Delta\nu$ in Hz) of these two exchanging signals at 21 °C and their coalescence temperature (T_c). It was confirmed that the magnitudes of the $\Delta G^{\ddagger}_c$ values obtained from the coalescence of the bridgehead proton signals and those from the exo-proton signals were in good agreement (e.g., in the case of **1c**, the values of $\Delta G^{\ddagger}_c$ from bridgehead proton signals and from exo-proton signals were 19.6 and 19.7 kcal/mol, respectively).

The rotational barriers ($\Delta G^{\ddagger}_c$) of *N*-thiobenzoyl derivatives **1a**, **2a**, and **3a** in nitrobenzene-d_5 were 20.7, 20.2 and 18.6 kcal/mol, respectively (Table 2). The $\Delta G^{\ddagger}_c$ values of the thioamides are larger than those of the corresponding amides (e.g., **4a**, 15.3 and **5a**, 16.9 kcal/mol, respectively), which is consistent with the general trend.[1,2] There is a good linear relationship in the Hammett plot between the magnitude of $\Delta G^{\ddagger}_c$ and σ_p^+ values[17] (r = 0.98, ρ^+ = 1.15 (**1a**−**1h**) and r = 0.99 and ρ^+ = 1.41 (**2a**−**2h**), see Figure S10 in Supporting Information); the substituent on the benzene ring showed a significant electronic effect on the rotational barrier ($\Delta G^{\ddagger}$) of the thioamides. A similar linear relationship was found in the cases of the corresponding

(14) Stewart, W. E.; Siddall, T. H., III. *Chem. Rev.* **1970**, *70*, 517–551.
(15) Oki, M. *Applications of Dynamic NMR Spectroscopy to Organic Chemistry*; VCH Publishers: Deerfield, 1985; Vol. 4.
(16) Ammann, C.; Meier, P.; Merbach, A. E. *J. Magn. Reson.* **1982**, *46*, 319–321.
(17) Hansch, C.; Leo, A.; Taft, R. W. *Chem. Rev.* **1991**, *91*, 165–195.
(18) Regression coefficients (r) and regression slopes (ρ^+) of corresponding amides are as follows (see ref 11): r = 0.98, ρ^+ = 0.61 for **4** and r = 0.99 and ρ^+ = 0.82 for **5**.

TABLE 2. Experimental Data and Barriers for Thioamide Bond Rotation Obtained by the Coalescence Method in Nitrobenzene-d_5

compound	R	T_c (°C)	$\Delta\nu$ (Hz)	$\Delta G_c^{\ddagger}$ [a]
1a[b]	H	148	68.0	20.7
1a[b,c]	H	(141)	(99.3)	(20.0)
1b	$N(CH_3)_2$	128	382.6	18.3
1c	OMe	157	442.1	19.6
1d	CH_3	174	491.1	20.3
1e	Cl	178	497.4	20.5
1f[b]	COOMe	149	44.9	21.1
1g[b]	CN	148	49.3	21.0
1h[b]	NO_2	143	24.4	21.3
2a	H	158	238.6	20.2
2a[c]	H	(149)	(274.5)	(19.6)
2b	$N(CH_3)_2$	96	171.5	17.4
2c	OMe	130	198.0	18.9
2d	CH_3	148	224.1	19.7
2e	Cl	154	214.8	20.0
2f	COOMe	169	211.5	20.8
2g	CN	168	219.9	20.7
2h	NO_2	171	212.4	20.9
3a	H	123	192.5	18.6
3a[c]	H	(111)	(215.4)	(18.0)

[a] Values in kcal mol^{-1}. The error of the coalescence temperature is ±1.0 °C and therefore the error of $\Delta G^{\ddagger}_c$ is ±0.05 kcal mol^{-1}. [b] Values were obtained from the coalescence of exo-proton signals, because the coalescence temperature for bridgehead proton signals exceeds 180 °C. [c] Values in parentheses were obtained in *o*-dichlorobenzene-d_4.

bicyclic amides (**4**) and the corresponding monocyclic amides (**5**), both having much smaller regression slopes.[18] Thus, while a more electron-withdrawing group tends to increases the amide/thioamide rotational barriers, the dependency of the magnitude of the rotational barriers on the electronic nature of the substituent is more significant in the case of the thioamides as compared with the corresponding amides.

The free energy of activation ($\Delta G^{\ddagger}$), and its components, the enthalpy of activation ($\Delta H^{\ddagger}$) and the entropy of activation ($\Delta S^{\ddagger}$) were also obtained experimentally by line shape analysis (Table 4). Rate constants were obtained at six different temperatures (Table 3), and then activation parameters $\Delta G^{\ddagger}$, $\Delta H^{\ddagger}$ and $\Delta S^{\ddagger}$ were obtained by least-squares analysis of the Eyring plots (see Figure S11 in Supporting Information).

The magnitude of $\Delta G^{\ddagger}$, especially at higher temperature (at 150 °C; $\Delta G^{\ddagger}_{150\,°C}$), was in good agreement with that of $\Delta G^{\ddagger}_c$ because the coalescence temperatures (T_c) of the thioamides ranged between 96−180 °C in this study, and the average value is around 150 °C. Since the magnitude of $\Delta S^{\ddagger}$ is affected by several factors, such as solvation upon thioamide rotation,[19] the $\Delta H^{\ddagger}$ value is likely a more appropriate index to estimate the energetic cost of rotation of thioamides, i.e., the N−C(S) double bond character, in this case. Indeed, the consistently large negative $\Delta S^{\ddagger}$ term contributes to the increase of the barrier ($\Delta G^{\ddagger}$ and probably $\Delta G^{\ddagger}_c$) in the cases of the bicyclic thioamides.

Experimentally, on the basis of the observed $\Delta H^{\ddagger}$ values for thioamide rotation, the energetic costs of rotation of the bicyclic thioamides (**1a**−**1h**) were smaller than those of the corresponding monocycles (**2a**−**2h**), particularly in nitrobenzene (Table 4).[20] Furthermore, the rotational barrier ($\Delta H^{\ddagger}$) of an acyclic thioamide, *N*,*N*-dimethylthiobenzamide (**3a**), is definitely smaller

TABLE 3. Estimated Rate Constants for Thioamide Bond Rotation Obtained from Line Shape Analysis of the Spectra in Nitrobenzene-d_5 and *o*-Dichlorobenzene-d_4

	T (K)	k (Hz)		T (K)	k (Hz)		T (K)	k (Hz)
				nitrobenzene-d_5				
1a	399	54.87	**2a**	397	66.36	**3a**	362	49.33
	410	102.06		406	109.33		372	93.85
	421	173.74		414	192.46		381	188.52
	431	308.33		422	318.20		390	314.96
	442	529.01		430	489.99		400	553.94
	453	896.63		437	704.00		409	950.26
1b	363	99.02	**2b**	346	83.78			
	373	172.82		355	162.67			
	382	296.39		363	281.70			
	392	490.10		372	483.68			
	401	837.17		379	722.78			
	410	1409.35		386	1166.80			
1c	363	38.49	**2c**	375	55.26			
	375	55.98		382	100.69			
	387	120.31		389	166.01			
	399	191.78		397	302.48			
	412	331.31		406	551.16			
	423	555.88		414	908.70			
1d	389	58.99	**2d**	382	40.35			
	399	90.26		392	76.31			
	409	148.92		401	144.77			
	420	247.46		409	244.16			
	429	407.11		417	400.14			
	438	676.48		426	622.80			
1e	393	52.06	**2e**	393	61.65			
	408	119.31		401	97.42			
	419	194.91		409	166.11			
	428	313.85		417	266.62			
	438	548.30		426	412.50			
	449	864.39		434	646.11			
1f	403	58.02	**2f**	403	67.24			
	413	84.68		412	93.84			
	420	115.01		420	145.25			
	422	125.07		429	243.47			
	431	189.13		438	431.99			
	442	295.88		448	706.73			
1g	403	58.21	**2g**	399	43.18			
	413	91.76		408	76.14			
	421	124.22		416	127.39			
	430	197.29		424	208.86			
	441	312.65		433	333.31			
	453	533.43		441	498.71			
1h	399	50.57	**2h**	399	37.78			
	410	85.22		408	64.65			
	420	118.31		417	107.52			
	430	198.22		427	182.18			
	441	319.58		436	308.73			
	453	474.38		446	498.71			
				o-dichlorobenzene-d_4				
1a	413	142.88	**2a**	385	38.94	**3a**	358	77.19
	420	213.10		393	67.65		367	149.69
	427	334.29		401	132.60		376	281.60
	434	551.16		409	241.64		385	454.62
	440	789.47		417	414.32		393	738.80
	444	961.44		426	640.37		401	1182.73

than that of monocyclic **2a** in both solvents.[21] This small rotational barrier ($\Delta H^{\ddagger}$) of **3a** can be interpreted in terms of twisting of the thioamide bond arising from 1,3-allylic strain between methyl hydrogens and the sulfur atom or the phenyl ring, which was observed in the solid-state structure of **3a** (see Table 1). Twisting of the thioamide bond leads to destabilization of the ground-state structure and therefore reduction of the

(19) Olsen, R. A.; Liu, L.; Ghaderi, N.; Johns, A.; Hatcher, M. E.; Mueller, L. J. *J. Am. Chem. Soc.* **2003**, *125*, 10125–10132.

(20) The fact that the negative entropic contribution is larger in more polar nitrobenzene than in *o*-dichlorobenzene can be partially explained in terms of enhanced solvation of thioamides, especially of the bicyclic thioamides, upon rotation. As for solvent effects on thioamide rotation, see: Wiberg, K. B.; Rush, D. J. *J. Am. Chem. Soc.* **2001**, *123*, 2038–2046.

(21) This observation is consistent with a previous study of the corresponding amides, i.e., monocyclic and acyclic amides. (a) Pinto, B. M.; Grindley, T. B.; Szarek, W. A. *Magn. Reson. Chem.* **1986**, *24*, 323–331. (b) Suarez, C.; Nicholas, E. J.; Bowman, M. R. *J. Phys. Chem. A* **2003**, *107*, 3024–3029.

TABLE 4. Experimental Rotational Barriers of Thioamides Obtained by Line Shape Analysis[a]

	R	$\Delta G^{\ddagger}_{25\,°C}$ [b]	$\Delta G^{\ddagger}_{150\,°C}$ [b]	$\Delta H^{\ddagger}$ [b]	$\Delta S^{\ddagger}$ [c]
1a	H	19.8 ± 0.5	20.6 ± 0.6	17.8 ± 0.3	−6.7 ± 0.7
1a[d]	H	(20.8 ± 1.0)	(20.3 ± 1.1)	(21.8 ± 0.6)	(3.5 ± 1.3)
1b	$N(CH_3)_2$	17.7 ± 0.4	18.5 ± 0.5	16.0 ± 0.2	−6.0 ± 0.6
1c	OMe	17.8 ± 1.0	19.8 ± 1.1	13.2 ± 0.5	−15.6 ± 1.4
1d	CH_3	19.0 ± 1.0	20.2 ± 1.1	15.9 ± 0.6	−10.2 ± 1.4
1e	Cl	19.3 ± 0.4	20.4 ± 0.5	16.7 ± 0.3	−8.7 ± 0.6
1f	COOMe	18.9 ± 0.5	20.9 ± 0.6	14.1 ± 0.3	−16.1 ± 0.7
1g	CN	19.3 ± 0.6	20.9 ± 0.7	15.4 ± 0.4	−13.0 ± 0.9
1h	NO_2	18.9 ± 0.7	20.9 ± 0.8	14.3 ± 0.4	−15.6 ± 0.9
2a	H	20.1 ± 0.6	20.2 ± 0.6	19.9 ± 0.3	−0.8 ± 0.8
2a[d]	H	(20.4 ± 0.9)	(19.7 ± 1.0)	(21.9 ± 0.5)	(5.2 ± 1.2)
2b	$N(CH_3)_2$	17.2 ± 0.3	17.5 ± 0.4	16.7 ± 0.2	−1.9 ± 0.4
2c	OMe	19.6 ± 0.4	18.8 ± 0.5	21.6 ± 0.2	6.5 ± 0.6
2d	CH_3	19.8 ± 0.3	19.8 ± 0.3	19.7 ± 0.2	0.0 ± 0.4
2e	Cl	19.7 ± 0.4	20.1 ± 0.4	18.7 ± 0.2	−3.3 ± 0.5
2f	COOMe	20.0 ± 1.3	20.7 ± 1.5	18.5 ± 0.8	−5.2 ± 1.8
2g	CN	20.3 ± 0.3	20.6 ± 0.4	19.6 ± 0.2	−2.4 ± 0.5
2h	NO_2	20.2 ± 0.4	20.8 ± 0.5	18.6 ± 0.2	−5.2 ± 0.5
3a	H	18.4 ± 0.5	18.7 ± 0.5	17.8 ± 0.3	−2.1 ± 0.7
3a[d]	H	(17.8 ± 0.2)	(18.1 ± 0.3)	(17.1 ± 0.1)	(−2.3 ± 0.3)

[a] Parameters were obtained from unbiased estimates of the standard deviations of least-squares parameters and are reported at the 95% confidence level. Values were obtained in nitrobenzene-d_5 unless otherwise noted. [b] Values in kcal mol^{-1}. [c] Values in eu (cal mol^{-1} K^{-1}). [d] Values in parentheses were obtained in *o*-dichlorobenzene-d_4.

rotational barrier. The present structural arguments are consistent with the minimum energy structures of **1a**, **2a**, and **3a**, which were obtained by calculation with DFT methods (see Table S1 in Supporting Information). While there is a tendency that the degrees of nitrogen-pyramidalization of the calculated structures are consistently larger than those of the solid-state structures,[11] **1a** showed significant nonplanarity ($\alpha = 158.1°$ and $|\tau| = 13.2°$) as compared with **2a** ($\alpha = 171.5°$ and $|\tau| = 7.3°$), and the twist angle of **3a** ($|\tau| = 13.0°$) was as large as that of **1a** (see Table S4 in Supporting Information). Also, the calculated rotational barriers ($\Delta H^{\ddagger}$)[22] of these thioamides in PCM models ($\epsilon = 35.6$, equivalent to nitrobenzene) showed that the rotational barriers ($\Delta H^{\ddagger}$) of the bicyclic thioamides (**1**) are consistently smaller than those of the monocyclic thioamides (**2**) (Table S2 in Supporting Information). Calculated $\Delta H^{\ddagger}$ values of the bicyclic thioamides (**1**) showed a good linear relationship with σ_p^+ values of the substituents (Figure S12).[23] Therefore, our findings are experimentally and theoretically consistent with the postulate that the structures of the bicyclic thioamides also show more significant nonplanarity than those of monocyclic thioamides in solution, and the degree of planarity depends on the electronic nature of the substituent.

The data found here is consistent with the idea that the relative contributions from resonance B versus resonance D control the planarity of the nitrogen. Only resonance B requires the nitrogen to be planar (pyramidalization and twisting will destabilize the C=N bond). Tying the nitrogen into a bicyclic structure pyramidalizes nitrogen and decreases the contribution from resonance B (increasing A and D). Strongly electron-withdrawing substituents (R) at the *para* position destabilize resonance D (increasing A and B), thereby increasing planarity. The difference between bicyclic amides and thioamides may be due to the difference between the relative proportions of resonance B in the overall resonance hybrid structures.[5,24]

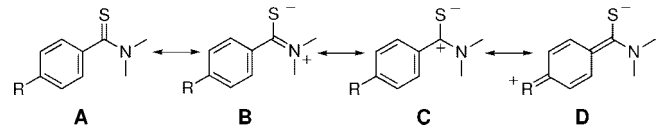

Conclusions

In summary, X-ray crystallographic study of some *N*-thioaroyl derivatives of secondary amines showed that thioamide derivatives of bicyclic 7-azabicyclo[2.2.1]heptane take significantly more nonplanar structures, as compared to the corresponding monocyclic thioamides. The magnitude of enthalpy of activation ($\Delta H^{\ddagger}$) for rotation about the N−C(S) bond, which was derived from dynamic NMR spectroscopy, showed reduced N−C(S) bond order in the bicyclic thioamides (**1a**−**1h**) and the acyclic thioamide **3a**, which is consistent with more nonplanar thioamide structures in solution. Therefore, nonplanar thioamides can be derived from the bicyclic 7-azabicyclo[2.2.1]heptane skeleton. On the basis of the substituent effects on the crystal structures and the magnitude of rotational barriers of the relevant bicyclic thioamides, the planarity of these compounds depends significantly on the electronic nature of the substituent, both in the solid phase and in solution.

Experimental Section

1. Synthetic Methods. General Procedure. *N*-Thiobenzoyl-7-azabicyclo[2.2.1]heptane (1a). A solution of *N*-benzoyl-7-azabi-

(22) ΔH is equal to the difference of potential energy *E* plus *RT*, zero-point energy, and the thermal corrections. Thus, it is well accepted that $\Delta H^{\ddagger}$ is approximately equal to ΔE (which is obtained by calculation) along the reaction coordinate. See: Houk, K. N.; Li, Y.; Evanseck, J. D. *Angew. Chem., Int. Ed. Engl.* **1992**, *31*, 682–708.

(23) The planarity (in terms of α value) of the calculated structures of the thioamides was also dependent on the electron-withdrawing nature of the aromatic substituents. In the case of the bicyclic thioamides **1**: **1h** (R = NO_2) 160.7° > **1g** (R = CN) 160.1° > **1f** (R = COOMe) 159.8° > **1e** (R = Cl) 158.8° > **1a** (R = H) ≈ **1d** (R = CH_3) 158.1° > **1c** (R = OMe) 157.2° > **1b** (R = $N(CH_3)_2$) 156.0°. In the case of the monocyclic **2**: **2h** (R = NO_2) 172.5° > **2g** (R = CN) ≈ **2f** (R = COOMe) 172.0° > **2e** (R = Cl) 171.3° ≈ **2a** (R = H) 171.5° ≈ **2d** (R = CH_3) 171.2° > **2c** (R = OMe) 170.3° > **2b** (R = $N(CH_3)_2$) 169.5°. The dependency of **2** was smaller than that of **1**, which was consistent with the trend found in the crystal structures. See Table S1 in Supporting Information.

(24) We thank an anonymous reviewer for valuable comment about the contribution of resonance structure D.

cyclo[2.2.1]heptane **3a** (262 mg, 1.30 mmol) and Lawesson's reagent (299 mg, 0.739 mmol) in dry toluene (25 mL) was refluxed for 3 h under Ar. The solvent was evaporated and the residue was flash-chromatographed (*n*-hexane/CH_2Cl_2 = 2:3) to give **1a** (197 mg, 70%) as a yellow solid. Mp: 112.1−113.0 °C (yellow cubes, recrystallized from CH_2Cl_2/*n*-hexane). ^{1}H NMR ($CDCl_3$, 400 MHz): δ 7.43−7.40 (2H, m), 7.38−7.31 (3H, m), 5.34 (1H, t, J = 5.0 Hz), 4.17 (1H, t, J = 5.0 Hz), 2.16−2.08 (2H, m), 1.95−1.87 (2H, m), 1.67−1.57 (4H, m). ^{13}C NMR ($CDCl_3$, 100 MHz): δ 194.0, 142.7, 129.3, 128.1, 126.4, 61.0, 59.0, 29.9, 27.5. Anal. Calcd for $C_{13}H_{15}NS$: C, 71.84; H, 6.96; N, 6.44. Found: C, 71.83; H, 6.97; N, 6.36.

Compound 1b. Mp: 165.0−166.5 °C (orange cubes, recrystallized from CH_2Cl_2/*n*-hexane). ^{1}H NMR ($CDCl_3$, 400 MHz): δ 7.45 (2H, d, J = 8.8 Hz), 6.62 (2H, d, J = 8.8 Hz), 5.30 (1H, t, J = 5.0 Hz), 4.40 (1H, t, J = 4.8 Hz), 3.00 (6H, s), 2.13−2.09 (2H, m), 1.96−1.90 (2H, m), 1.63−1.52 (4H, m). ^{13}C NMR ($CDCl_3$, 100 MHz): δ 194.9, 151.6, 130.1, 129.2, 110.6, 61.5, 59.4, 40.2, 30.0, 27.5. Anal. Calcd for $C_{15}H_{20}N_2S$: C, 69.19; H, 7.74; N, 10.76. Found: C, 69.11; H, 7.81; N, 10.63.

Compound 1c. Mp: 127.2−128.4 °C (yellow needles, recrystallized from CH_2Cl_2/*n*-hexane). ^{1}H NMR ($CDCl_3$, 400 MHz): δ 7.43 (2H, d, J = 8.8 Hz), 6.85 (2H, d, J = 8.8 Hz), 5.31 (1H, t, J = 5.2 Hz), 4.28 (1H, t, J = 4.8 Hz), 3.83 (3H, s), 2.15−2.05 (2H, m), 1.94−1.86 (2H, m), 1.65−1.55 (4H, m). ^{13}C NMR ($CDCl_3$, 100 MHz): δ 194.2, 160.7, 135.2, 128.7, 113.2, 61.3, 59.3, 55.4, 30.0, 27.5. Anal. Calcd for $C_{14}H_{17}NOS$: C, 67.98; H, 6.93; N, 5.66. Found: C, 68.16; H, 6.87; N, 5.66.

Compound 1d. Mp: 131.6−133.0 °C (yellow needles, recrystallized from CH_2Cl_2/*n*-hexane). ^{1}H NMR ($CDCl_3$, 400 MHz): δ 7.33 (2H, d, J = 8.4 Hz), 7.14 (2H, d, J = 8.4 Hz), 5.33 (1H, t, J = 5.0 Hz), 4.23 (1H, t, J = 4.8 Hz), 2.36 (3H, s), 2.15−2.08 (2H, m), 1.94−1.87 (2H, m), 1.66−1.54 (4H, m). ^{13}C NMR ($CDCl_3$, 100 MHz): δ 194.3, 139.9, 139.6, 128.7, 126.7, 61.1, 59.1, 29.9, 27.5, 21.2. Anal. Calcd for $C_{14}H_{17}NS$: C, 72.68; H, 7.41; N, 6.05. Found: C, 72.84; H, 7.47; N, 6.09.

Compound 1e. Mp: 157.8−159.0 °C (yellow cubes, recrystallized from CH_2Cl_2/*n*-hexane). ^{1}H NMR ($CDCl_3$, 400 MHz): δ 7.37 (2H, d, J = 8.4 Hz), 7.32 (2H, d, J = 8.4 Hz), 5.31 (1H, t, J = 5.2 Hz), 4.16 (1H, t, J = 4.8 Hz), 2.15−2.08 (2H, m), 1.93−1.88 (2H, m), 1.67−1.55 (4H, m). ^{13}C NMR ($CDCl_3$, 100 MHz): δ 192.7, 141.0, 135.3, 128.3, 127.9, 61.2, 59.1, 29.9, 27.5. Anal. Calcd for $C_{13}H_{14}ClNS$: C, 62.02; H, 5.60; N, 5.56. Found: C, 62.06; H, 5.59; N, 5.60.

Compound 1f. Mp: 132.2−133.4 °C (yellow plates, recrystallized from CH_2Cl_2/*n*-hexane). ^{1}H NMR ($CDCl_3$, 400 MHz): δ 8.02 (2H, d, J = 8.4 Hz), 7.46 (2H, d, J = 8.4 Hz), 5.34 (1H, t, J = 4.8 Hz), 4.08 (1H, t, J = 5.0 Hz), 3.93 (3H, s), 2.16−2.08 (2H, m), 1.93−1.87 (2H, m), 1.68−1.55 (4H, m). ^{13}C NMR ($CDCl_3$, 100 MHz): δ 192.6, 166.3, 146.5, 130.5, 129.5, 126.3, 61.1, 59.0, 52.2, 29.9, 27.5. Anal. Calcd for $C_{15}H_{17}NO_2S$: C, 65.43; H, 6.22; N, 5.09. Found: C, 65.28; H, 6.32; N, 5.01.

Compound 1g. Mp: 194.6−195.5 °C (yellow cubes, recrystallized from AcOEt/*n*-hexane). ^{1}H NMR ($CDCl_3$, 400 MHz): δ 7.65 (2H, d, J = 8.0 Hz), 7.49 (2H, d, J = 8.0 Hz), 5.32 (1H, t, J = 5.0 Hz), 4.05 (1H, t, J = 4.8 Hz), 2.15−2.09 (2H, m), 1.93−1.87 (2H, m), 1.70−1.58 (4H, m). ^{13}C NMR ($CDCl_3$, 100 MHz): δ 191.1, 146.3, 132.0, 126.9, 118.1, 112.6, 61.2, 59.1, 29.8, 27.4. Anal. Calcd for $C_{14}H_{14}N_2S$: C, 69.39; H, 5.82; N, 11.56. Found: C, 69.51; H, 5.95; N, 11.46.

Compound 1h. Mp: 216.3−217.2 °C (yellow cubes, recrystallized from AcOEt). ^{1}H NMR ($CDCl_3$, 400 MHz): δ 8.22 (2H, d, J = 8.8 Hz), 7.54 (2H, d, J = 8.8 Hz), 5.34 (1H, t, J = 5.0 Hz), 4.05 (1H, t, J = 4.8 Hz), 2.17−2.10 (2H, m), 1.94−1.88 (2H, m), 1.71−1.59 (4H, m). ^{13}C NMR ($CDCl_3$, 100 MHz): δ 190.9, 148.0, 147.8, 127.2, 123.6, 61.3, 59.1, 29.9, 27.5. Anal. Calcd for $C_{13}H_{14}N_2O_2S$: C, 59.52; H, 5.38; N, 10.68. Found: C, 59.47; H, 5.40; N, 10.61.

Compound 2a. Mp: 73.0−73.8 °C (pale yellow plates, recrystallized from CH_2Cl_2/*n*-hexane). ^{1}H NMR ($CDCl_3$, 400 MHz): δ 7.37−7.30 (5H, m), 3.97 (2H, t, J = 7.2 Hz), 3.46 (2H, t, J = 6.8 Hz), 2.11−2.04 (2H, m), 1.99−1.93 (2H, m). ^{13}C NMR ($CDCl_3$, 100 MHz): δ 197.1, 143.9, 128.6, 128.2, 125.5, 53.7, 53.3, 26.4, 24.5. Anal. Calcd for $C_{11}H_{13}NS$: C, 69.07; H, 6.85; N, 7.32. Found: C, 68.99; H, 6.79; N, 7.24.

Compound 2b. Mp: 113.2−114.5 °C (yellow needles, recrystallized from CH_2Cl_2/*n*-hexane). ^{1}H NMR ($CDCl_3$, 400 MHz): δ 7.39 (2H, d, J = 8.8 Hz), 6.62 (2H, d, J = 8.8 Hz), 3.98 (2H, t, J = 7.0 Hz), 3.62 (2H, t, J = 6.8 Hz), 2.98 (6H, s), 2.10−2.03 (2H, m), 1.98−1.91 (2H, m). ^{13}C NMR ($CDCl_3$, 100 MHz): δ 197.7, 151.0, 131.5, 128.1, 110.9, 54.2, 53.9, 40.2, 26.6, 24.7. Anal. Calcd for $C_{13}H_{18}N_2S$: C, 66.62; H, 7.74; N, 11.95. Found: C, 66.80; H, 7.78; N, 11.81.

Compound 2c. Mp: 111.0−112.5 °C (colorless needles, recrystallized from CH_2Cl_2/*n*-hexane). ^{1}H NMR ($CDCl_3$, 400 MHz): δ 7.37 (2H, d, J = 9.0 Hz), 6.86 (2H, d, J = 9.0 Hz), 3.97 (2H, t, J = 7.0 Hz), 3.82 (3H, s), 3.53 (2H, t, J = 6.6 Hz), 2.10−2.04 (2H, m), 2.00−1.95 (2H, m). ^{13}C NMR ($CDCl_3$, 100 MHz): δ 197.1, 160.0, 136.4, 127.7, 113.4, 55.3, 53.9, 53.7, 26.5, 24.7. Anal. Calcd for $C_{12}H_{15}NOS$: C, 65.12; H, 6.83; N, 6.33. Found: C, 65.06; H, 6.98; N, 6.27.

Compound 2d. Mp: 72.5−73.8 °C (yellow needles, recrystallized from CH_2Cl_2/*n*-hexane). ^{1}H NMR ($CDCl_3$, 400 MHz): δ 7.27 (2H, d, J = 8.0 Hz), 7.15 (2H, d, J = 8.0 Hz), 3.97 (2H, t, J = 7.0 Hz), 3.49 (2H, t, J = 6.8 Hz), 2.34 (3H, s), 2.11−2.04 (2H, m), 1.99−1.92 (2H, m). ^{13}C NMR ($CDCl_3$, 100 MHz): δ 197.5, 141.2, 138.8, 128.8, 125.7, 53.8, 53.4, 26.4, 24.6, 21.2. Anal. Calcd for $C_{12}H_{15}NS$: C, 70.20; H, 7.36; N, 6.82. Found: C, 70.21; H, 7.36; N, 6.84.

Compound 2e. Mp: 95.7−96.8 °C (yellow cubes, recrystallized from CH_2Cl_2/*n*-hexane). ^{1}H NMR ($CDCl_3$, 400 MHz): δ 7.32 (4H, s), 3.96 (2H, t, J = 7.0 Hz), 3.46 (2H, t, J = 6.8 Hz), 2.11−2.05 (2H, m), 2.00−1.95 (2H, m). ^{13}C NMR ($CDCl_3$, 100 MHz): δ 195.8, 142.2, 134.7, 128.5, 127.1, 53.8, 53.5, 26.5, 24.6. Anal. Calcd for $C_{11}H_{12}ClNS$: C, 58.53; H, 5.36; N, 6.20. Found: C, 58.41; H, 5.49; N, 6.16.

Compound 2f. Mp: 120.3−121.8 °C (yellow needles, recrystallized from AcOEt/*n*-hexane). ^{1}H NMR ($CDCl_3$, 400 MHz): δ 8.03 (2H, d, J = 8.4 Hz), 7.41 (2H, d, J = 8.4 Hz), 3.97 (2H, t, J = 7.0 Hz), 3.92 (3H, s), 3.42 (2H, t, J = 6.8 Hz), 2.13−2.06 (2H, m), 2.02−1.95 (2H, m). ^{13}C NMR ($CDCl_3$, 100 MHz): δ 195.8, 166.4, 147.8, 130.1, 129.8, 125.6, 53.6, 53.3, 52.2, 26.4, 24.5. Anal. Calcd for $C_{13}H_{15}NO_2S$: C, 62.62; H, 6.06; N, 5.62. Found: C, 62.61; H, 6.09; N, 5.54.

Compound 2g. Mp: 151.4−152.2 °C (yellow cubes, recrystallized from CH_2Cl_2/*n*-hexane). ^{1}H NMR ($CDCl_3$, 400 MHz): δ 7.65 (2H, d, J = 8.8 Hz), 7.44 (2H, d, J = 8.8 Hz), 3.95 (2H, t, J = 7.0 Hz), 3.41 (2H, t, J = 6.8 Hz), 2.14−2.06 (2H, m), 2.04−1.97 (2H, m). ^{13}C NMR ($CDCl_3$, 100 MHz): δ 194.4, 147.6, 132.3, 126.3, 118.2, 112.2, 53.6, 53.3, 26.5, 24.5. Anal. Calcd for $C_{12}H_{12}N_2S$: C, 66.63; H, 5.59; N, 12.95. Found: C, 66.68; H, 5.86; N, 12.93.

Compound 2h. Mp: 155.2−156.1 °C (yellow plates, recrystallized from CH_2Cl_2/*n*-hexane). ^{1}H NMR ($CDCl_3$, 400 MHz): δ 8.23 (2H, d, J = 8.8 Hz), 7.51 (2H, d, J = 8.8 Hz), 3.98 (2H, t, J = 7.0 Hz), 3.43 (2H, t, J = 6.6 Hz), 2.15−2.08 (2H, m), 2.06−1.99 (2H, m). ^{13}C NMR ($CDCl_3$, 100 MHz): δ 194.0, 149.3, 147.4, 126.5, 123.8, 53.6, 53.3, 26.5, 24.5. Anal. Calcd for $C_{11}H_{12}N_2O_2S$: C, 55.91; H, 5.12; N, 11.86. Found: C, 55.91; H, 5.15; N, 11.86.

Compound 3a. Mp: 66.0−66.8 °C (yellow cubes, recrystallized from CH_2Cl_2/*n*-hexane). ^{1}H NMR ($CDCl_3$, 400 MHz): δ 7.37−7.28 (5H, m), 3.60 (3H, s), 3.16 (3H, s). ^{13}C NMR ($CDCl_3$, 100 MHz): δ 201.1, 143.2, 128.5, 128.2, 125.6, 44.0, 43.1. Anal. Calcd for $C_9H_{11}NS$: C, 65.41; H, 6.71; N, 8.48. Found: C, 65.43; H, 6.75; N, 8.37.

2. Dynamic NMR. In variable-temperature NMR experiments, temperatures were calibrated by a standard method using ethylene glycol.[14,16]

Line shape analysis was carried out with a program, DNMR (Bruker Biospin) and was performed by iterative matching of simulated spectra with the experimental spectra.

X-ray Crystallographic Analysis. Data collections were performed using a CCD area detector diffractometer with Mo Kα radiation in a *w*-scan mode ($l = 0.71073$ Å). The structure was solved by direct methods and refined by full-matrix least-squares refinements based on F^2. All hydrogen atoms were anisotropically refined. Hydrogen atoms were added geometrically and refined with a riding model. Structure solutions were performed with the SHELXS-97 and SHELXL-97.[25]

Acknowledgment. This work was supported by a Grant-in-Aid for Scientific Research from the Japan Society for the Promotion of Science.

Supporting Information Available: ^{1}H and ^{13}C NMR spectra, crystallographic data in CIF format, figures showing dynamic NMR, and details of calculations. This material is available free of charge via the Internet at http://pubs.acs.org.

JO801996B

(25) Sheldrick, G. M. *Acta Crystallogr.* **2008**, *A64*, 112–122.